Failure analysis of buried cast iron water main using fracture mechanics

Suborno Debnath, & Ashutosh Sutra Dhar
Department of Civil Engineering – Memorial University of Newfoundland, St. John's, NL, Canada

ABSTRACT
Water main failure, particularly for cast iron pipes, has been identified as a major concern for municipalities, as a number of water main breaks occur every year. Despite numerous past studies, pipe failure mechanisms observed in the field are not well understood. Conventional analyses using continuum based and Winkler spring based finite element methods calculate higher circumferential stress on the pipe wall which might lead to longitudinal wall cracking. However, circumferential cracking is the most commonly observed failure mode in water mains. In this paper, fracture mechanics is applied to study the stress concentrations in the buried pipe and offer new insights into the failure mechanisms of buried pipelines. Stress intensity factors for cast iron water mains with different shapes of corrosion defects are investigated using finite element analysis for crack assessment of the pipelines. The stress intensity factors are compared with the fracture toughness determined from laboratory tests.

Keywords: Water main, Cast iron pipe, Stresses intensity factor, Failure mechanisms, Fracture mechanics, Finite-element analysis

RÉSUMÉ

La principale défaillance des conduites d'eau, en particulier pour les tuyaux en fonte, a été identifiée comme une préoccupation majeure pour les municipalités, étant donné qu'un certain nombre de bris de conduites d'eau se produisent chaque année. Malgré de nombreuses études antérieures, les mécanismes de rupture des conduites observés sur le terrain ne sont pas bien compris. Les analyses conventionnelles utilisant des méthodes d'éléments finis à base de continuum et de ressorts de Winkler calculent une contrainte circonférentielle plus élevée sur la paroi de la conduite, ce qui peut conduire à une fissuration de la paroi longitudinale. Cependant, la fissuration circonférentielle est le mode de rupture le plus couramment observé dans les conduites d'eau. Dans cet article, la mécanique de la rupture est appliquée pour étudier les concentrations de contraintes dans le tuyau enterré et offrir de nouvelles perspectives sur les mécanismes de défaillance des pipelines enfouis. Les facteurs d'intensité des contraintes pour les canalisations d'eau en fonte présentant différentes formes de défauts de corrosion sont étudiés à l'aide d'une analyse par éléments finis pour l'évaluation des fissures des canalisations. Les facteurs d'intensité de contrainte sont comparés à la ténacité à la rupture déterminée à partir d'essais en laboratoire.

Mots clés: Conduite d'eau, Conduite en fonte, Facteur d'intensité des contraintes, Mécanismes de rupture, Mécanique de la rupture, Analyse par éléments finis

1 INTRODUCTION

Buried pipelines are used to transport drinking water, waste water or other fluids. There are different kinds of pipe materials used to carry water. Gray cast iron is one of them, which was generally installed in Canada in the middle of the 19th century. The aged pipes show deterioration and are prone to failure. Rajani et al. (1995) estimated that approximately 50% of water mains were gray cast iron, in their survey of 21 cities in Canada. Gray cast iron shows a tendency to corrode in the buried condition and may create corrosion pits which cause stress concentration around the pits. According to Folkman (2012), nearly 75 percent of all utilities have corrosive soil conditions. Corrosion is thus considered one of the main reasons for water main failure in Canada and the USA. Due to water main failure, 50% of the water has been reportedly lost in the city of Mount Pearl, Canada, which causes huge economic loss (Frick and Manuel, 2005). Cast iron water mains may fail due to circumferential cracking, longitudinal cracking, joint failure or blowouts (Rajani et at, 1996). Circumferential failures mainly occur due to corrosion pits and it is the most common mode of failure for water distribution networks (Makar et al, 2005). Liyanage and Dhar (2015, 2017) showed that the stress concentration can be higher in the circumferential direction than the longitudinal direction around a pit of a pipe that is subjected to non-uniform bedding, which may create cracks in the longitudinal direction. The failure of the pipe occurs when the applied stresses in the pipe exceed the capacity of the pipe material (Gould et al, 2011). Trickey et al. (2016) showed that circumferential cracking in water mains may be caused due to longitudinal bending that results from non-uniform bedding support or a frost load in the soil above the pipe. Differential soil movement occurs due to frost penetration, which causes ring failure. The lack of ground support causes additional stresses on the pipe wall near the unsupported zone (Balkaya et al. 2012). Pipe stresses are significantly affected by leaks opening, which may exceed the material strength and may fail in the vicinity of an opening where stress increases exponentially with the increase of crack length (Cassa et al, 2009). Dhar et al. (2004) revealed that the lack of soil support within a localized zone can lead to stress or strain concentration in flexible pipes. The stress or strain concentration was higher for pipes with higher stiffness relative to the soil (Dhar et al. 2004). Although these approaches are widely used to assess pipeline failure, fracture mechanics has not been extensively applied to investigate the failure of a pipeline. In fracture mechanics, the stress intensity factor (SIF) is generally used for the assessment of brittle fracture. The stress intensity factor was found to provide less error and is a more accurate way than using stress concentration for failure assessment (Dipen et al. 2015).

Limited research information is currently available in the literature on circumferential crack assessment in water mains using fracture mechanics. Some recent papers on stress intensity factor show that for a surface crack, the maximum stress intensity factor occurs at different points, leading to different modes of failure, because the type of loading affects the stress intensity factors (Li and Yang, 2012). However, no study on the effect of pit shape and non-uniform bedding with various lengths is available in the literature. In this paper, a three-dimensional finite element analysis is developed to determine the stress intensity factor for different shapes of corrosion pits of a cast iron water main that is supported by non-uniform bedding. A three-dimensional finite-element analysis is also performed to calculate the stress intensity factor of cast iron and compare it with the lab results, which helps to understand the failure mechanism.

2 FRACTURE TOUGHNESS FROM LABORATORY TESTS

Single-edge notch beam (SENB) tests were conducted in the lab by the research group at Memorial University of Newfoundland (Ali, 2017) with 3.2 mm, 4.7 mm and 6 mm pre-crack notches (V-notch) using ASTM E 1820-01(2001) where the width to depth ratio (W/B) of the specimens was kept in the range of $1 < W/B < 2$. In those tests, a simple chevron (V) notch was used rather than a complex straight through notch, recommended in the ASTM standards (Figure 1). The main advantage of using a V notch is that the fabrication procedure is easier. Figure 2 shows the specimen used in SENB tests.

The clear span (S), depth (W) and thickness (B) of the specimen were 84 mm, 14 mm and 7 mm, respectively. Three-point loading was applied on the specimen and a linear voltage displacement transducer (LVDT) was attached to measure the displacement. The width of the V notch was 2.4 mm. The failure load was recorded for each specimen. Details of the test procedure are available in Ali, (2017). Fracture toughness K_c was then calculated from the failure load and crack length (ASTM E 1820-01, 2001) using the following equation Eq. (1).

$$Kc = \frac{PS}{BW^{3/2}} \, f(a/w) \qquad [1]$$

where $f(a/w) = \frac{3\,(a/w)^{1/2}}{2\,(1 + 2\,a/w)(1 - a/w)^{3/2}} * [1.99 - (a/w) * (1 - a/w) * (2.15 - 3.93 * a/w + 2.7 * a^2/w^2)$

and *P* is the ultimate load, *S* is the clear span, *B* is the thickness, *a* is the crack length and *w* is the depth.

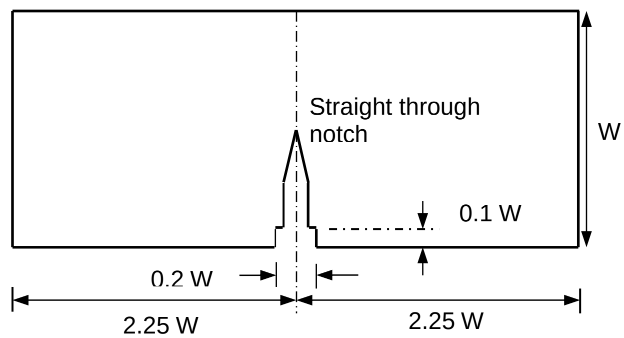

Figure 1. ASTM E 1820-01 recommended specimen

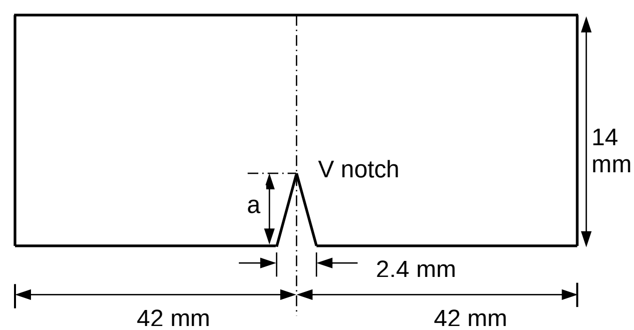

Figure 2. Test specimen used

However, Eq. (1) is recommended in the ASTM standards for the specimen shape shown in Figure 1. To validate the applicability of Eq. (1), a 3D finite element model is developed using Abaqus to determine the fracture toughness of the specimen in the single-edge notch beam (SENB) tests. The cast iron specimen is defined as a 3D deformable solid body. For FE modeling, an 8-node linear brick element (C3D8R) is used. A Young's modulus of 121 GPa and Poisson's ratio of 0.25 are considered in this model, based on the data reported in Ali, (2017). The specimen is simply supported. The clear span (S), depth (W), and thickness (B) of the specimen are 84 mm, 14 mm and 7 mm, respectively. Pre-crack notches (V-notch) of 3.2 mm, 4.7 mm and 6 mm depth are considered as crack lengths. The width of the V notch is 2.4 mm. Figure 3 shows the finite element mesh considered in the model.

The contour integral method is used to determine the fracture toughness where the crack extension direction is along the normal to the crack plane. For each integral, five contours are specified. Figure 4 shows the crack extension direction.

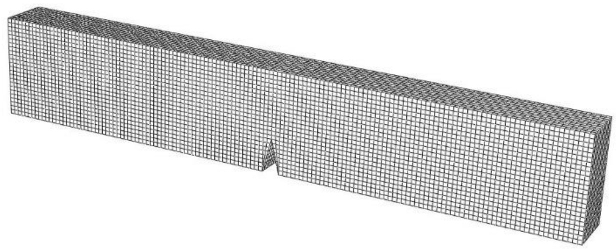

Figure 3. 3D finite element modeling of single-edge notch beam (SENB) test

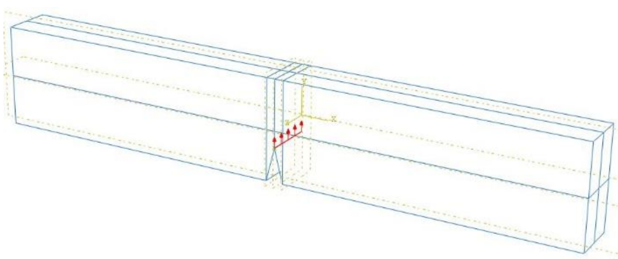

Figure 4. Crack extension direction in Contour integral method

The failure load is taken from single-edge notch beam (SENB) tests to determine the fracture toughness and deflection using finite element analysis. In finite element modeling, a finer mesh typically results in a more accurate solution than coarser mesh. However, as a mesh is made finer, the computation time increases. Therefore, a mesh convergence analysis is performed to increase speed and obtain sufficient accuracy and to ensure that the result is no longer dependent on mesh size. The h-method (varying the element size) is implemented. Stress intensity factors calculated from finite element analysis are compared with the test results obtained using Eq. (1), as shown in Table 1 and Figure 5.

Table 1. Fracture toughness, Kc from tests and Numerical model

Specimen	Failure Load (N)	Crack Length (mm)	Kc Test (MPa√m)	Kc Abaqus (MPa√m)
SB1	1869	3.2	17.16	16.80
SB2	2106	3.2	19.33	18.93
SB3	1191	4.7	14.39	14.81
SB4	1068	4.7	12.91	13.35
SB5	1020	4.7	12.33	12.70
SB6	1523	4.7	18.40	19.01
SB7	1179	6.0	18.34	18.75
SB8	1136	6.0	17.67	17.80

The fracture toughness of cast iron varies between 12 to 19 MPa√m (Figure 5) where the maximum deflection is 19 mm (Figure 6). The fracture toughness obtained from Abaqus is almost identical with the test value, indicating that Eq. (1) is applicable for a simple chevron (V) notch, which can be used instead of the complex straight through notch. Finite element calculations of deflections also match the measurements (Figure 6). Finite element models thus reasonably represent the test conditions.

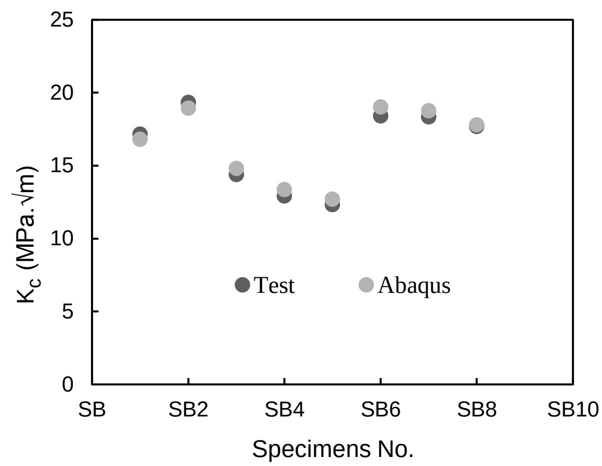

Figure 5. Comparison of fracture toughness from test and Abaqus

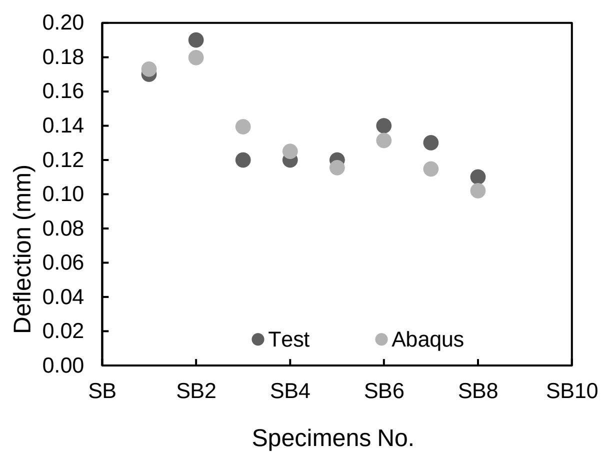

Figure 6. Comparison of deflection from test and Abaqus

3 FINITE ELEMENT MODELING OF CAST IRON WATER MAIN

Three-dimensional finite element analyses are carried out using Abaqus to obtain the pipe stress distribution and stress intensity factor of the pipe. The model is developed so that the pipeline and the soil model are defined as 3D deformable solid bodies. An 8-node linear brick element (C3D8R) is used. First, an extended finite element method is used to determine the crack propagation direction. The contour integral method is used to determine the stress intensity factor around the corrosion pit, for which the crack direction needs to be assigned. For the contour integral method, the crack extension direction is defined along the normal to the crack plane and for each integral, five contours are specified. Figure 7 shows the crack extension direction applied, obtained from finite element analysis, discussed later in this paper. Soil load, internal pressure, surcharge (snow load) and traffic load affect the cast iron pipeline, which is buried in an elastoplastic soil.

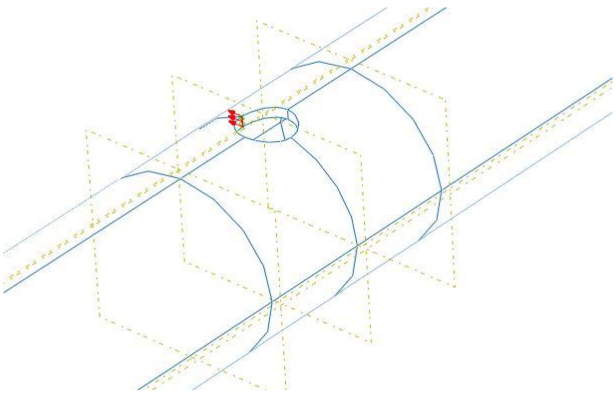

Figure 7. Crack extension direction in Contour integral method

Lack of ground support is also considered using a void (Figure 8). For soil, two boundary conditions are used and for pipeline, one boundary conditions is considered. Longitudinal displacements of soil and pipe are restrained at the end plane by roller support, because an infinite or semi-infinite medium of soil can be assumed to move in a vertical direction. The bottom surface of the 3D finite-element soil model is required to be completely fixed in order to restrain horizontal and vertical movement. The diameter of the cast iron is assumed to be 175 mm and the thickness is 10 mm, buried in a medium dense soil with 2 m of soil cover. The pipe is subjected to 400 kN/m^2 internal pressure. Gravity load, snow load (25 kN/m^2) and truck load (axle load 14400 kg) are also considered in the model. Gravity load is calculated manually and applied as a pressure at the top of the soil in the contour integral method.

The length of the pipe considered is 4 m. The corrosion pit is located at the invert position of the pipe. Uniform bedding, as well as a non-uniform bedding condition, are considered. To simulate the non-uniform bedding condition, a 1 m or 2 m long, 50 mm thick void is provided at the invert of the pipe. Circular, elliptical and diamond types of corrosion pit are considered, where the diameter of the circular pit is 50 mm, the length of the major axis is 50 mm for the elliptical pit and the diagonal length is 50 mm for the diamond shaped corrosion pit. The void at the bedding is symmetrical to the pit hole and extends 90° or 180° around the pit circumference. The FE model is first validated through simulation of data available in the literature (Liyanage and Dhar, 2017). Soil parameters reported in Liyanage and Dhar (2017) are employed in the analyses. A parametric study is conducted to investigate the influence of the dilation angle in order to select a suitable dilation angle. The dilation angle is varied from 8º to 15º and no significant variation in SIF is found. Table 2 summarizes the material parameters used in the analysis.

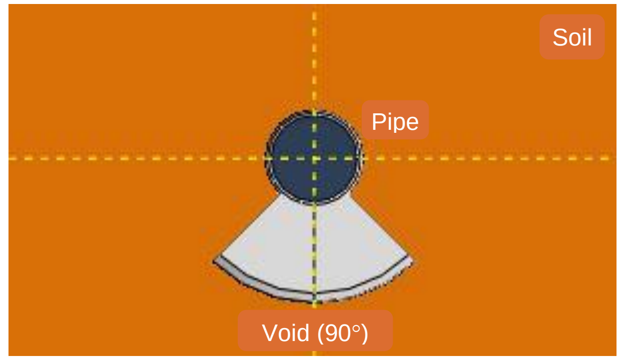

Figure 8. Symmetric void (90°) with respect to pit hole

Table 2. Material Parameters

Material Properties	Soil	Cast Iron
Density (kN/m^3)	1.77	7.88
Young's modulus (MPa)	24	138,000
Poisson's Ratio	0.25	0.21
Friction Angle in (°)	38	-
Dilation Angle in (°)	15	-
Cohesion Yield Stress (kPa)	0.01	
Max Principal Stress (MPa)	-	180
Tolerance	-	0.05

4 RESULTS

As discussed earlier, in the contour integral method for calculating stress intensity factor, the direction of crack propagation has to be defined. To understand the direction of stress propagation, an extended finite element method (XFEM) is employed using Abaqus. In XFEM, the maximum principal stress criterion is used to identify the direction of crack propagation. Figure 9 shows the direction of crack propagation for a pipe with a circular corrosion pit. The pit is located at the invert of the pipe where a 2 m long void which extends 90° around the pit circumference, in the bedding soil. To ensure initiation and propagation of the crack, a high pressure (i.e. 400 kPa) is applied at the ground surface. Figure 9 demonstrates that a crack initiates and propagates in the circumferential direction of the pipe.

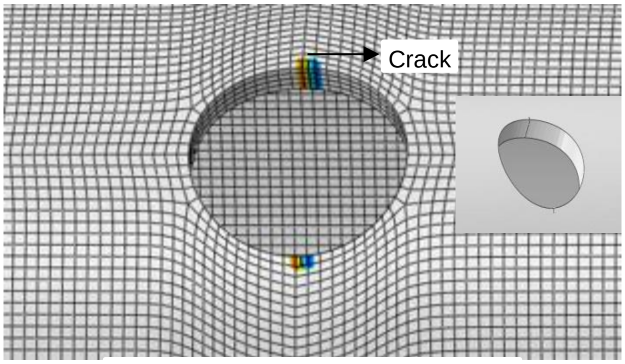

← Longitudinal direction of the pipe →

Figure 9. Crack propagation direction (philsm)

The distribution of major principal stress around the circular pit is plotted in Figure 10. Since cracking is generated by tension, the major principal stress from Abaqus provides the direction of cracking. Figure 10 shows the highest tensile stress along the circumferential direction of the pipe across the circular corrosion pit. Thus, cracking is expected in the circumferential direction of the pipe due to high longitudinal stress, which is consistent with the crack direction observed in Figure 9.

Maximum principal stress distribution (MPa)

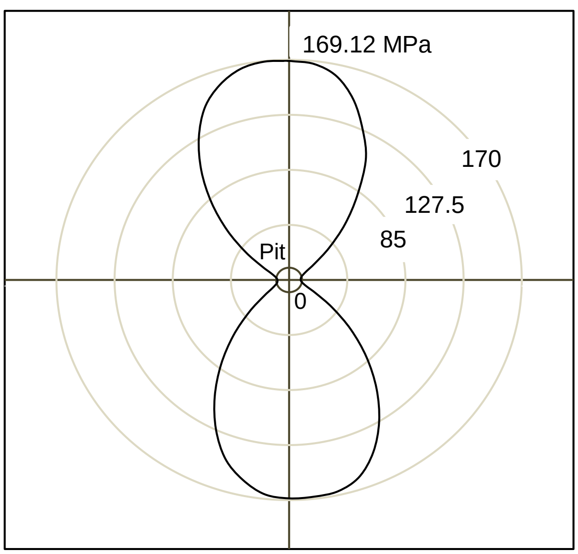

← Longitudinal direction of the pipe →

Figure 10. Distribution of maximum principal stress around a circular pit

To determine the direction of crack initiations and propagations for different shapes of corrosion pits, the contours of major principal stress are plotted against the pit in Figures 11 to 13. These figures demonstrate high tensile stress (red colour in the figure) in the circumferential direction of the pipe. Therefore, crack directions along the circumference are assigned in the contour integral method, as shown in Figure 7.

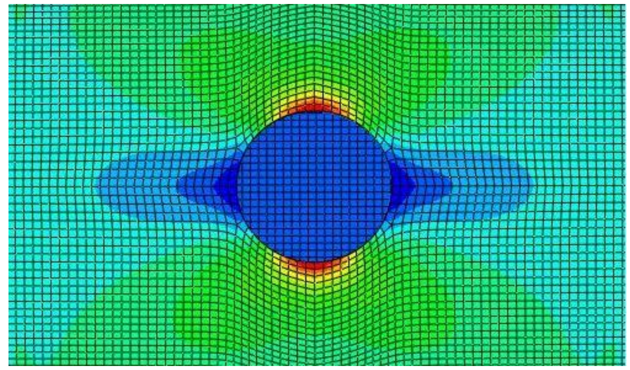

← Longitudinal direction of the pipe →

Figure 11. Maximum principal stress around a circular pit

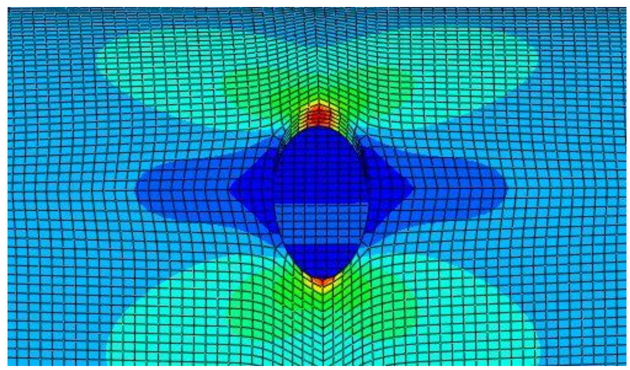

← Longitudinal direction of the pipe →

Figure 12. Maximum principal stress around an elliptical pit

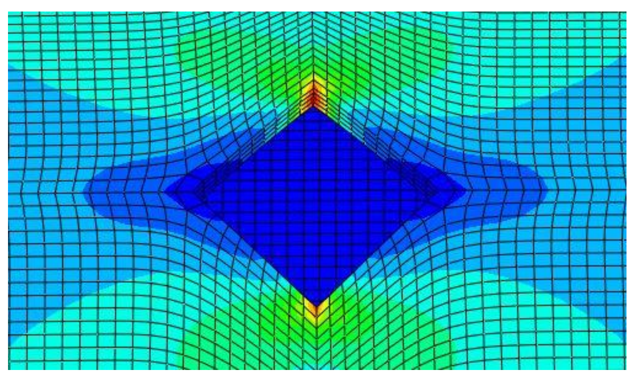

← Longitudinal direction of the pipe →

Figure 13. Maximum principal stress around a diamond shaped pit

The stress intensity factors (SIFs) calculated using finite element analysis, for different pipe installation and loading conditions are shown in Tables 3 to 5. The SIFs in the tables suggest that the SIF is highest for a diamond shaped corrosion pit and lowest for the circular shape. The SIF for the elliptical corrosion pit lies between the diamond and circular corrosion pits. The SIF increases with the decrease of tip radius of the corrosion hole. SIF increases due to gravity, surcharge (snow load) and traffic load but decreases due to internal pressure. SIF increases 40 % due to traffic load and decreases 6% due to internal pressure for the 1 m hole under the pit. Thus, for fracture, the critical condition is when the cast iron water main is empty and has internal pressure.

However, the SIFs under typical loading conditions of water mains (Tables 3 to 5) are less than the fracture toughness determined for cast iron pipe materials shown in Table 1. The maximum calculated SIF (i.e. 6.80 MPa√m) is about 45% of the mean value of the fracture toughness (i.e. 15 MPa√m). A crack may propagate at values of SIF that can be substantially below fracture toughness, which is known as subcritical crack growth, stable cracking or quasi-static crack propagation, due to stress corrosion. Strained bonds at crack tips are weakened due to the chemical action of environmental factors like water that facilitate crack growth during stress corrosion (Atkinson, 1984). Cullin et al (2014) reported that subcritical corrosion fatigue is one of the threats to gray cast iron water pipes which is mainly due to the cyclic load. A casting defect may cause a microscopic crack on the pipe's interior that may accelerate crack propagation and failure may occur before fracture toughness is reached.

Table 3. Stress intensity factor in MPa√m (1m hole under the pit and extending 90° around the pit circumference)

Shape of the pit	Gravity and Surcharge	Gravity, Surcharge and Traffic	Gravity, Surcharge, Traffic and Internal pressure
Circular	0.56	0.77	0.72
Elliptical	1.37	1.91	1.79
Diamond	2.49	3.48	3.29

Table 4. Stress intensity factor in MPa√m (2m hole under the pit and extending 90° around the pit circumference)

Shape of the pit	Gravity and Surcharge	Gravity, Surcharge and Traffic	Gravity, Surcharge, Traffic and Internal pressure
Circular	0.56	0.77	0.66
Elliptical	1.44	2.09	1.97
Diamond	2.62	3.81	3.64

Table 5. Stress intensity factor in MPa√m (2m hole under the pit and extending 180° around the pit circumference)

Shape of the pit	Gravity and Surcharge	Gravity, Surcharge and Traffic	Gravity, Surcharge, Traffic and Internal pressure
Circular	0.99	1.38	1.22
Elliptical	2.71	3.77	3.67
Diamond	4.91	6.80	6.65

5 CONCLUSION

In this study, finite element analysis is used to calculate stress intensity factors for a pipeline subjected to corrosion pits. Stress intensity factors are compared with fracture toughness, determined from laboratory tests for fracture assessment of a cast iron water main. A finite element method is used to determine the fracture toughness of the cast iron specimen and compared with the single-edge notch beam (SEBN) tests results. In this study, a simple chevron (V) notch is used instead of a complex straight through notch, which is recommended by ASTM E 1820-01. From those results, the conclusion can be drawn that a complex straight through notch can be successfully replaced with a chevron (V) notch that will reduce fabrication difficulty.

The study of buried cast iron water mains under various loading conditions subjected to non-uniform bedding demonstrates that the pipe SIF is significantly affected by pit shape and the erosion void at the bedding. The SIF is higher in the circumferential direction than in the longitudinal direction across the corrosion pit. As a result, crack propagation is expected along the circumferential direction. Three corrosion pit shapes (circular, diamond and elliptical) are considered in this paper. The round hole corrosion pit is the safest among the three types of corrosion pits, and the diamond shape is the least safe. SIF increases with the gravity, surcharge (snow load) and traffic load but decreases due to internal pressure. Although the SIF does not exceed the fracture toughness for the pipe considered, it may fail due to subcritical crack growth. This study can be extended by investigating the effect of subcritical crack growth in a cast iron water main.

6 ACKNOWLEDGEMENTS

Funding of this research project was provided by the Natural Sciences and Engineering Research Council of Canada (NSERC) through its Collaborative Research and Development Grants and the city of Mount Pearl in the province of Newfoundland and Labrador. This financial support is gratefully acknowledged.

7 REFERENCES

Ali I. 2017. "Mechanical properties of an exhumed cast iron pipe material". M.Sc. Thesis, Memorial University, Newfoundland and Labrador, Canada.

ASTM E1820-01 2001. "Standard test method for measurement of fracture toughness." *American society for testing and materials.*

Atkinson B. K. 1984. "Subcritical crack growth in geological materials." *Journal of Geophysical Research*, vol. 89, no. B6: 4077-4114.

Balkaya, M., Moore, I. D., and Sağlamer, A. 2012. "Study of Nonuniform Bedding Support Because of Erosion under Cast Iron Water Distribution Pipes." *Journal of Geotechnical and Geoenvironmental Engineering*, 138(10): 1247–1256.

Cassaa A.M., Zylb J.E. van and Laubsche R.F. 2010. "A numerical investigation into the effect of pressure on holes and cracks in water supply pipes." *Urban Water Journal*, Vol. 7, No. 2: 109–120.

Cullin M. J., Petersen T.H. and Paris A. P.E. 2015. "Corrosion Fatigue Failure of a Gray Cast Iron Water Main". Journal of *Pipeline Systems Engineering* and *Practice*,6(2):05014003.DOI:10.1061/(ASCE)PS.1949 1204.0000188.

Dhar, A. S., Moore, I. D., & McGrath, T. J. 2004. "Two-dimensional analyses of thermoplastic culvert deformations and strains." *Journal of Geotechnical and Geoenvironmental Engineering*, ASCE, 130(2): 199-208.

Dipen B., Ketul B. and Dipal P. 2015. "Stress Concentration Factor Converts Into Stress Intensity Factor Using ANSYS." *European Journal of Advances in Engineering and Technology*, 2015, 2(1): 46-49.

Folkman S. 2012. "Water Main Break Rates in the USA and Canada: A Comprehensive Study." *Research Report, Utah State University Buried Structures Laboratory*, Logan, UT, USA.

Frick, G.R. and Manuel, J. 2005. "Leak Detection Program: The City of Mount Pearl", Proc. Leakage 2005, Halifax, NS, Canada

Gould, S.J.F., Boulaire, F.A., Burn, S., Zhao, X.L. & Kodikara, J.K., 2011, Seasonal factors influencing the failure of buried water reticulation pipes*, Water Science & Technology:* 2692-2699.

Li C.Q., Yang S.T. 2012. "Stress intensity factors for high aspect ratio semi-elliptical internal surface cracks in pipes." *International Journal of Pressure Vessels and Piping* 96-97: 13-23.

Liyanage, K., and Dhar, A. S. 2015. "Three Dimensional Finite Element Analyses of Partially Supported Water Mains." *68th Canadian Geotechnical Conference*. Quebec City, Canada.

Liyanage, K., and Dhar, A. S. 2017. "Stresses in Cast Iron Water Main Subjected to Non-Uniform Bedding and Localized Concentrated Forces". In press.

Liyanage, K.T.H and Dhar, A.S. 2017. "Effects of corrosion pits on the wall stresses in cast iron water mains." *ASCE Journal of Pipeline Systems - Engineering and Practice*, 8(4): 04017023.

Makar, J. M., Rogge, R., McDonald, S., and Tesfamariam, S. 2005. "The Effect of Corrosion Pitting on Circumferential Failures in Grey Iron Pipes." American Water Works Association, Denver.

Rajani B. and McDonald S. 1995. *Water mains break data on different pipe materials for 1992 and 1993*. Report No. A-7019.1, National Research Council, Ottawa, ON.

Rajani, B., Zhan, C. and Kuraoka, S. 1996. "Pipe Soil Interaction Analysis of Jointed Water Mains." *Canadian Geotechnical Journal* 33 (3): 393–404. Doi: 10.1139/t96- 061.

Trickey, S. A., Moore, I.D. and Balkaya, M. 2016. "Parametric study of frost-induced bending moments in buried cast iron water pipes", *Tunnelling and Underground Space Technology* 51: 291-300.